Robustness Analysis of Model Predictive Control for Constrained Image-Based Visual Servoing

Shahab Heshmati-alamdari, George K. Karavas, Alina Eqtami, Michael Drossakis and Kostas J. Kyriakopoulos

***Abstract*— In this paper, robustness analysis of constrained Image Based Visual Servoing based on Nonlinear Model Predictive Control (NMPC) is presented. It is known, that real applications such an aerial or a fast underwater robotic systems, suffer from the presence of external disturbances. These kinds of disturbances are inevitable in the physical systems, so it is of great interest to employ robust controllers. Therefore, a rigorous robustness analysis should be conducted. In this paper, the Image Based Visual Servoing system under the MPC framework is proven to be Input-to-State Stable (ISS) and a permissible upper bound of the disturbances is provided. Finally, the validity of the theoretic results is illustrated through a simulated example.**

I. INTRODUCTION

Over the last decades, visual servoing has gained a lot of research interest in motion control systems. In general, it employs the visual information of a camera as feedback to determine the required control signal. Structurally, visual servoing can be classified as: (i) Position-Based Visual Servoing (PBVS), where the visual features extracted from the image are used to estimate the $3D$ pose of the robot wrt the target; (ii) Image-Based Visual Servoing (IBVS), where the control inputs are determined directly on the $2D$ image plane based on the error of the image features between the current and desired images, and (iii) Hybrid Visual Servoing, where $3D$ PBVS is combined with $2D$ IBVS [1], [2].

In this paper, the IBVS scheme is considered, as it is more effective than the other two, owing to its inherent robustness against camera calibration imperfections. However, handling constraints is yet another issue of consideration. Constraints in this particular systems are, *inter alia*, the visibility constraints imposed from the fact that the target must be in the field-of-view of the camera during the motion of the robot, [3], or the $3D$ constraints of the physical system, such as actuator limits and nonholonomic constraints. In view of the difficulty to handle hard constraints, different methods have been developed. More specifically, in [4] and [5] path planning strategies on the features in the image plane have been proposed and in [6] a path planning algorithm via LMI optimization has been studied.

An approach for effectively handling constraints for real time applications is via Nonlinear Model Predictive Control, due to its inherent virtues [7],[8]. The IBVS via NMPC framework has been studied in [9], [10], [11], [12]. In [10], the Visual Predictive Control (VPC) scheme has been proposed in which the workspace limitations, the visibility constraints and the actuators limits are formulated as state, output, and input constraints. The image based obstacle avoidance problem for an UAV using NMPC was tackled in [13].

Other issues for consideration are the external disturbances and the uncertainties of the system. For real applications in robotic systems, such as controlling underwater vehicles, model uncertainties and external disturbances are inevitable. Notice, that in [14], the authors provided a robustness stability analysis for the classical IBVS controller with respect to (wrt) the depth parameter. In this work, the absence of the depth parameters is introduced to the system as a disturbance. In the aforementioned IBVS via NMPC frameworks only nominal stability has been considered. In particular in [10], in the simulation part the authors have considered noise in the parameters of the visual features. However, no robustness analysis was performed. In this paper, a rigorous robustness analysis of the IBVS via NMPC is conducted and additionally a permissible upper bound of the disturbances is derived. Regarding the stability analysis of IBVS, it is worth mentioning that only local asymptotic stability can be obtained for classical IBVS [1]. For that reason, in this paper, only local stability analysis is considered. Moreover, the analysis will be using the Input-to-State Stability (ISS) notion, due to the persistent disturbances which leads to ultimate boundedness results. More specifically, the ISS stability wrt disturbances of the overall framework is proven and it has been shown that the visual features on the image plane are converging to a bounded terminal set that includes the desired position of the visual features on the image plane. Some relevant works on robust NMPC for general nonlinear systems are, [15], [16].

The remainder of the paper is organized as follows. The mathematical modeling of the IBVS as well as the problem statement, are presented in Section II. Section III, accommodates the main results of the paper namely the robustness analysis of the NMPC for image based visual servoing. Furthermore, this analysis leads to the determination of the permissible upper bound of the disturbances. In Section IV, the simulation results are presented. Finally, the section V summarizes the results of this paper and indicates further research endeavors.

Shahab Heshmati-alamdari, George K. Karavas, Michael Drossakis and Kostas J. Kyriakopoulos are with the Control Systems Lab, Department of Mechanical Engineering, National Technical University of Athens, 9 Heroon Polytechniou Street, Zografou 15780, Greece {shahab,mc06101,dross,kkyria@mail.ntua.gr}.
Alina Eqtami is with Cardiovascular Surgery, Childrens Hospital Boston, Harvard Medical School, Boston MA, 02115, USA. {alina.eqtami@childrens.harvard.edu}.

II. Problem Formulation

A. Mathematical Modelling

In this section, the mathematical formulation of the image based visual servoing problem is presented for a pinhole camera model. The model of the IBVS is going to be utilized for the solution of the optimal control problem of the NMPC.

Let $[X_c, Y_c, Z_c]^\top$ be the axes of the camera frame $\mathcal{C}$ attached at the center of the camera O_c. The coordinates of the image frame $\mathcal{I}$ are given by $[u, v]^\top$ with O_I denoting the center of the image, as depicted in Fig.1. Notice that the Z_c axis of the camera frame is perpendicular to the image plane transversing O_I. A $3D$ point $P = [x, y, z]^\top$ wrt the

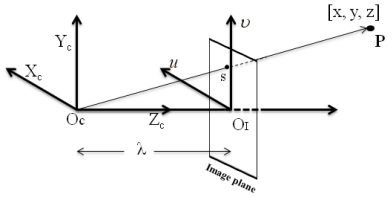

Fig. 1. The coordinate frame of the camera system.

camera frame will appear in the image plane as a $2D$ image feature $s = [u, v]^\top$ with coordinates [1]:

$$s = \begin{bmatrix} u \\ v \end{bmatrix} = \frac{\lambda}{z} \begin{bmatrix} x \\ y \end{bmatrix} \tag{1}$$

where λ is the focal length of the camera as it is shown in Fig.1. The time derivative of the coordinates of the fixed point P, during motion of the camera wrt the camera frame, are as follows [1]:

$$\dot{P} = -\Omega \times P - T \tag{2}$$

Let $V = \begin{bmatrix} T \\ \Omega \end{bmatrix} = [T_x, T_y, T_z, \omega_x, \omega_y, \omega_z]^\top$ denotes the translational and angular velocities of the camera. Using (1) and (2) the time derivative of the image feature in the image plane has the following vector form:

$$\dot{s} = L_s V \tag{3}$$

where:

$$L_s(u, v, z) = \begin{bmatrix} -\frac{\lambda}{z} & 0 & \frac{u}{z} & \frac{uv}{\lambda} & -\frac{\lambda^2+u^2}{\lambda} & v \\ 0 & -\frac{\lambda}{z} & \frac{v}{z} & \frac{\lambda^2+v^2}{\lambda} & -\frac{uv}{\lambda} & -u \end{bmatrix} \tag{4}$$

is called the interaction matrix L_s related to s. For controlling a 6 DOF motion, at least four image features must be available [1], thus using $n \geq 4$ image features, we obtain:

$$\begin{bmatrix} \dot{s_1} \\ \dot{s_2} \\ \vdots \\ \dot{s_n} \end{bmatrix} = \begin{bmatrix} Ł_{s_1} \\ Ł_{s_2} \\ \vdots \\ Ł_{s_n} \end{bmatrix} V \tag{5}$$

which represents the model of the overall system. The vector V is the control input of the system. For brevity, the state vector and interaction matrix of the system for n image features is denoted by $s = [s_1, s_2, \cdots, s_n]^\top$ and $L_s = [Ł_{s_1}, Ł_{s_2} \cdots, Ł_{s_n}]^\top$, respectively. The Newton-Euler method is used for approximating (5), in order to obtain the model of the system in the discrete-time frame:

$$s_{k+1} = s_k + dt(\widehat{L}_{s_k} \cdot V_k) \tag{6}$$

with dt to be the sampling period. It is pointed out that the $\widehat{L}_{s_k}$ is depended on z parameter, thus two cases can be considered. In the first case, called *constant* z, the value of the z in the $\widehat{L}_{s_k}$ is replaced by its desired $z = z^*$ thus, the $\widehat{L}_{s_k}$ depends only on the values of the image features. Notice that in the case of *constant* z the stability results are locally and are sensible in a neighborhood around the desired z [14]. If the z parameter is available in each sampling time, is called the *known* z case. For the rest of paper we denote $s_k = [s_{(1,k)}, s_{(2,k)}, \cdots, s_{(n,k)}]^\top$ to be the vector of the state at a time-step k. The vector of the velocity of the camera $V_k = [T_{(x,k)} \quad T_{(y,k)} \quad T_{(z,k)} \quad \omega_{(x,k)} \quad \omega_{(y,k)} \quad \omega_{(z,k)}]^\top$ will denote the input of the system at a time-step k. The nominal system (6) can be written in stack vector form as:

$$s_{k+1} = f(s_k, V_k) \tag{7}$$

The requirements of system (7), also named as visibility constraints, ensure that the image feature s will not leave the image-plane during the control operation are given as:

$$\underline{u} \leq u \leq \bar{u} \tag{8a}$$

$$\underline{v} \leq v \leq \bar{v} \tag{8b}$$

where $\bar{u}$ and $\bar{v}$ are the maximum and $\underline{u}$ and $\underline{v}$ are the minimum pixels wrt u and v coordinates of the image-plane respectively. The state constraints (8a)-(8b) form the state constraint set $S_{set} \subseteq \mathbb{R}^{2n}$ i.e., $s_k \in S_{set}$. The control constraint set V_{set} is compact and it is given by:

$$V_k \in V_{set} \subseteq \mathbb{R}^6 \tag{9}$$

The constraints of the input are of the form $|T_x| \leq \bar{T}_x$, $|T_y| \leq \bar{T}_y$, $|T_z| \leq \bar{T}_z$, $|\omega_x| \leq \bar{\omega}_x$, $|\omega_y| \leq \bar{\omega}_y$ and $|\omega_z| \leq \bar{\omega}_z$. where $(\bar{\cdot})$ denotes the upper bound for each of the variables. We set $\|V_k\| \leq \bar{V}$, with $\bar{V}$to be the upper bound for the control input of the system. The nominal system (7) is Lipschitz continuous in S_{set} with Lipschitz constant $0 < C_f < \infty$. More specifically:

Lemma 1: The nominal model (7), subject to constraints (8a)-(8b) and (9), is locally Lipschitz in s for all $s_k \subseteq S_{set}$. For the case of *constant* z ($z = z^*$) the Lipschitz constant is defined as:

$$C_f \triangleq 5\sqrt{2} \max \left\{ 1, (\frac{dt\bar{T}_z}{z^*}), (\frac{2\sqrt{2}\bar{\omega}_x dt \max(\bar{u}\bar{v})}{\lambda}), \right.$$
$$\left., (\frac{2\sqrt{2}\bar{\omega}_y dt \max(\bar{u}\bar{v})}{\lambda}), (\frac{2dt\bar{\omega}_y\bar{u}}{\lambda}), (\frac{2dt\bar{\omega}_x\bar{v}}{\lambda}), (dt\bar{\omega}_z) \right\}$$

Also, for the case of *known* z ($z = z(t)$) the Lipschitz constant is defined as:

$$C_f \triangleq 5\sqrt{2} \max \left\{ 1, (\frac{dt\bar{T}_z\bar{u}}{z^*}), (\frac{2\sqrt{2}\bar{\omega}_x dt \max(\bar{u}\bar{v})}{\lambda}), (\frac{2dt\bar{\omega}_y\bar{u}}{\lambda}), \right.$$
$$\left., (\frac{2\sqrt{2}\bar{\omega}_y dt \max(\bar{u}\bar{v})}{\lambda}), (\frac{2dt\bar{\omega}_x\bar{v}}{\lambda}), (\frac{dt\lambda\bar{T}_x}{z^*}), (\frac{dt\lambda\bar{T}_y}{z^*}), (dt\bar{\omega}_z) \right\}$$

Note that this Lipschitz constant is independent of the number of the features in (7). Assume that system (7) is affected by disturbances whose vector form is: $\xi = [\xi_{(u,1)}, \xi_{(v,1)}, \cdots, \xi_{(u,n)}, \xi_{(v,n)}]^\top$. Therefore, a perturbed version of the system should be also considered:

$$s_{k+1} = f(s_k, V_k) + \xi_k \tag{10}$$

with $\xi \in \Xi \subset \mathbb{R}^{2n}$ and Ξ to be a compact set. Assume also, that $||\xi_k|| \leq \bar{\xi}$, where $\bar{\xi}$ is an upper bound for this set. This perturbation set is defined on the $2D$ image plane and can be written in the 3D Cartesian space using (1) as:

$$\begin{aligned} \frac{\lambda x}{z} - \bar{\xi} \leq \frac{\lambda x + dx}{z + dz} \leq \frac{\lambda x}{z} + \bar{\xi} \\ \frac{\lambda y}{z} - \bar{\xi} \leq \frac{\lambda y + dy}{z + dz} \leq \frac{\lambda y}{z} + \bar{\xi} \end{aligned} \tag{11}$$

where dx, dy and dz are the coordinates of the external disturbances wrt the camera frame in the $3D$ frame.

B. Control Design and Objective

The aim of this section is to control the real system (10) subject to the state constraints of (8a)-(8b) and the control constraints (9) to reach to a desired compact set that includes the desired state $s_d = [s_1 \quad s_2 \quad \cdots \quad s_n]^\top \in S_{set}$. It can be proven that, using a NMPC control law, the state of the system converges to this desired set. Inside this terminal set, an auxiliary terminal controller will be equipped to drive the system to the desired point, that could be a classic image based controller as the one used in [1]. The predictive controllers consist in solving iteratively an open-loop optimal control problem which is based on the actual state of the system s_k, at a sample time k, with respect to a control sequence $V_f(k)$ and provide an optimal control sequence $V_f^*(k)$. The optimal control problem of the NMPC is given:

$$\min_{V_f(k)} J_N(s_k, V_f(k)) = \tag{12a}$$

$$\min_{V_f(k)} \sum_{i=0}^{i=N-1} F(\hat{s}(k+i|k), V(k+i|k)) + E(\hat{s}(k+N|K))$$

subject to

$$\hat{s}(k+j|k) \in S_j, \qquad \forall j = 1, \ldots, N-1, \tag{12b}$$

$$V(k+j|k) \in V_{set}, \qquad \forall j = 0, \ldots, N-1, \tag{12c}$$

$$\hat{s}(k+N|k) \in \mathscr{E}_f \tag{12d}$$

where N denotes the prediction horizon, the set $\mathscr{E}_f$ is the terminal constrained set and F and E are the running and terminal cost functions, respectively. The vector $\hat{s}(k+j|k)$ denotes the predicted state of the nominal system (7) at sampling time $k+j$ with $j \geq 0$. The predicted state is based on the measurement of the state of the perturbed system s_k at a sampling time k, while using the nominal model and a sequence of control inputs $\{V_k, \ldots, V_{k+j-1}\}$. Therefore, it is: $\hat{s}(k+j|k) = f(\hat{s}(k+j-1|k), V_{k+j-1})$. Notice, that it holds $\hat{s}(k|k) = s_k$. Moreover, it is shown that the difference between the state sequence of the actual system (10) and the predicted sequence of the system, is in fact, bounded:

Lemma 2: The difference between the real state s_{k+j} at the time $k+j$ and the predicted state $\hat{s}(k+j|k)$ at the same time under the same control sequence, starting at the same initial state s_k is upper bounded by:

$$||s_{k+j} - \hat{s}(k+j|k)|| \leq \sum_{i=0}^{j-1} (C_f)^i \bar{\xi} \tag{13}$$

In Lemma 2, the difference between the real state trajectory of system (10) and the predicted state trajectory of the nominal system is given. To address this divergence, we used a restricted constrained set $S_j \subseteq S_{set}$ instead of the state constrained set S_{set} into (12b). For more details the reader is referred to [15] and [16]. This constraint tightening technique is utilized in order to guarantee that the evolution of the state of the perturbed system, when a control sequence computed by the NMPC is applied, will actually satisfy the state constrained set S_{set}. The cost function $F(\cdot)$ as well as the terminal cost $E(\cdot)$ are of quadratic form, i.e., $F(\hat{s}, V) = \hat{s}^\top Q \hat{s} + V^\top R V$ and $E(\hat{s}) = \hat{s}^\top P \hat{s}$, with P, Q and R to be positive definite matrices. Particulary we define $Q = diag\{q_1, q_2, \cdots, q_{(2n-1)}, q_{(2n)}\}$, $R = diag\{r_1, r_2, r_3, r_4, r_5, r_6\}$ and $P = diag\{p_1, p_2, \cdots, p_{(2n-1)}, p_{(2n)}\}$. For the running cost function F, it is easy to show that $F(0,0) = 0$, as well as:

Lemma 3: The cost function $F(s, V)$ is lower bounded by a $\mathcal{K}_\infty$-function. In particular:

$$F(s, V) \geq min(q_1, q_2, \cdots, q_{(2n-1)}, q_{(2n)}, r_1, r_2, \cdots, r_6)||s||^2 \tag{14}$$

Taking into account (8a)-(8b) and (9), it can be concluded that the sets S_{set} and V_{set} are bounded, thus the following result can be obtained:

Lemma 4: The cost function $F(s, V)$ is Lipschitz continuous in $S_{set} \times V_{set}$, with Lipschitz constant C_F, where:

$$C_F = 2(n(\bar{u}^2 + \bar{v}^2))^{\frac{1}{2}} \cdot \sigma_{max}(Q) \tag{15}$$

and $\sigma_{max}(Q)$ denotes the largest singular value of the Q.

Assumption 1: For the nominal system (7), there is an admissible positively invariant set $\mathscr{E} \subset S_{set}$ such that the terminal region $\mathscr{E}_f \subset \mathscr{E}$, where $\mathscr{E} = \{s \in S_{set} : ||s|| \leq \varepsilon_0\}$ with ε_0 being a positive parameter.

Assumption 2: We assume that in the terminal set $\mathscr{E}_f$, there is a local controller $V_k = h(s_k) \in V_{set}, \quad \forall s \in \mathscr{E}$ and an associated Lyapunov function E such that $E(f(s_k, h(s_k))) - E(s_k) + F(s_k, h(s_k)) \leq 0$.

Assumption 3: The associated Lyapunov function for the terminal region is Lipschitz in $\mathscr{E}$, with Lipschitz constant $C_E = 2\varepsilon_0 \sigma_{max}(P)$ for all $s \in \mathscr{E}$. Considering that from *Assumption 1* we have: $||s|| = (|u_1|^2 + |v_1|^2 + \cdots + |u_n|^2 + |v_n|^2)^{\frac{1}{2}} \leq \varepsilon_0$ for all $s \in \mathscr{E}$.

Assumption 4: Inside the set $\mathscr{E}$ we have $E(s) = s^T P s \leq \alpha_\varepsilon$, where $\alpha_\varepsilon = max\{p_1, p_2, \cdots, p_{(2n-1)}, p_{(2n)}\}\varepsilon_0^2 > 0$. Assuming that $\mathscr{E} = \{s \in S_{set(N-1)} : h(s) \in V_{set}\}$ and taking a positive parameter α_{ε_f} such that $\alpha_{\varepsilon_f} \in (0, \alpha_\varepsilon)$, we assume that the terminal set $\mathscr{E}_f = \{s \in \mathbb{R}^3 : E(s) \leq \alpha_{\varepsilon_f}\}$ is such that $\forall s \in \mathscr{E}$, $f(s, h(s)) \in \mathscr{E}_f$.

III. Input-to-State Stability for constrained IBVS-MPC

In this section the Input-to-State stability analysis for the closed-loop image based visual servoing (10) via NMPC will

be presented. We begin by denoting $V_F^*(k-1)$ as the optimal solution that results from (12a)-(12d) at a time-step $k-1$. We, also, denote a feasible control sequence $\tilde{V}(k+j|k)$ of the optimization problem at time-step k, such as:

$$\tilde{V}(k+j|k) = \begin{cases} V^*(k+j|k-1) & \text{for } j = 0, \dots, N-2 \\ h(\hat{q}(k+N-1|k)) & \text{for } j = N-1 \end{cases} \tag{16}$$

From (12c) and *Assumption 2* is clear that $\tilde{V}(k+j|k) \in V_{set}$.

A. Feasibility of constrained IBVS-MPC

At this point we want to find a bound $\bar{\xi}$ for the uncertainties, such as, if D_N is the set of states of the system where the MPC optimization problem is feasible, then the closed-loop system in D_N is stable. That means that if $s_k \in D_N$ then $s_{k+1} = f(s_k, V_k^*) + \xi_{k+1} \in D_N, \quad \text{for all} \quad \xi_{k+1} \in \Xi$.

Theorem 1: Consider the Image Based Visual Servo System of (10) that is subject to constraints (8a)-(8b) and (9). The Control input that provided by NMPC 12a-12d drives and stabilizes the image features vector s to a set $\mathscr{E}$ around the desired image features vector s^*, without violating the constraints, If and Only If the disturbances are bounded by:

$$\bar{\xi} \leq \frac{\alpha_\varepsilon - \alpha_{\varepsilon_f}}{C_E \cdot C_f^{N-1}} \tag{17}$$

Proof: First it will be shown that:

$$\begin{aligned} &||\hat{s}(k|k) - \hat{s}(k|k-1)|| = \xi_k \leq \bar{\xi} \\ &||\hat{s}(k+1|k) - \hat{s}(k+1|k-1)|| = \\ &= ||f(\hat{s}(k|k)) - f(\hat{s}(k|k-1))|| \\ &\leq C_f(||\hat{s}(k|k) - \hat{s}(k|k-1)||) \leq C_f \cdot \bar{\xi} \\ &\qquad \vdots \\ &||\hat{s}(k+N-1|k) - \hat{s}(k+N-1|k-1)|| \leq C_f^{N-1} \cdot \bar{\xi} \end{aligned}$$

From *Assumption 3* we have:

$$\begin{aligned} &E(\hat{s}(k+N-1|k)) - E(\hat{s}(k+N-1|k-1)) \leq \\ &\leq C_E||\hat{s}(k+N-1|k) - \hat{s}(k+N-1|k-1)|| \leq C_E \cdot C_f^{N-1} \cdot \bar{\xi} \end{aligned}$$

For the nominal system and based on the optimal solution $V^*(k+j|k-1)$ we have: $E(\hat{s}(k+N-1|k-1)) \in \mathscr{E}_f$. Therefore, taking into account *Assumption 4*:

$$E(\hat{s}(k+N-1|k)) \leq \alpha_{\varepsilon_f} + C_E \cdot C_f^{N-1} \cdot \bar{\xi}$$

we want $E(\hat{s}(k+N-1|k))$ to belong to the set $\mathscr{E}$, thus from *Assumption 4* it must satisfy $E(\hat{s}(k+N-1|k)) \leq \alpha_\varepsilon$, which leads to:

$$E(\hat{s}(k+N-1|k)) \leq \alpha_{\varepsilon_f} + C_E \cdot C_f^{N-1} \cdot \bar{\xi} \leq \alpha_\varepsilon$$

Therefore, if the uncertainties of the system are bounded by $\bar{\xi} \leq \frac{\alpha_\varepsilon - \alpha_{\varepsilon_f}}{C_E \cdot C_f^{N-1}}$ then $E(\hat{s}(k+N-1|k))$ belongs to the set $\mathscr{E}$, and from *Assumption 4* we get $E(\hat{s}(k+N|k)) \in \mathscr{E}_f$, which concludes the proof. ■

B. Convergence of constrained IBVS-MPC

In the following we will show that the states of the perturbed system are converging to the terminal set. Consider the optimal cost $J_N^*(k-1) = J^*(s_{k-1}, V^*(k-1))$ from (12a), at the time-step $(k-1)$ as a Lyapunov function candidate. Consider, also, the cost of the feasible sequence at time-step k as $\tilde{J}_N(k) = \tilde{J}(s_k, \tilde{V}(k))$. We denote by $\tilde{s}(k+i|k)$ the "feasible" state of the system which accounts for the predicted state at time-step $k+i$, based on the measurement of the real state at time-step k, when the feasible control sequence $\tilde{V}(k+i|k)$ from (16) is used. We want to show that in the feasible set of states, D_N, the closed loop of the image based visual servoing via NMPC is input to state stable for all $s \in D_N$. The difference between the optimal cost and the feasible cost is:

$$\begin{aligned} &\Delta J = \tilde{J}_N(k) - J_N^*(k-1) = \\ &= \sum_{i=0}^{i=N-1} F(\tilde{s}(k+i|k), \tilde{V}(k+i|k)) + E(\tilde{s}(k+N|k)) \\ &- \sum_{i=0}^{i=N-1} F(\hat{s}(k+i-1|k-1), V^*(k+i-1|k-1)) \\ &- E(\hat{s}(k+N-1|k-1)) = \sum_{i=0}^{i=N-2} F(\tilde{s}(k+i|k), \tilde{V}(k+i|k)) \\ &- F(\hat{s}(k+i|k-1), V^*(k+i|k-1)) \\ &+ F(\tilde{s}(k+N-1|k), \tilde{V}(k+N-1|k)) \\ &- F(\hat{s}(k-1|k-1), V^*(k-1|k-1)) \\ &+ E(\tilde{s}(k+N|k)) - E(\hat{s}(k+N-1|k-1)) \end{aligned}$$

where $\tilde{V}(k+N-1|k) = h(\hat{s}(k+N-1|k))$ taken from (16) and $\tilde{V}(k+i|k) = V^*(k+i|k-1)$ for $i = 0, \dots, N-2$. Also from *Lemma 4* combined with *Lemma 2* we get:

$$\begin{aligned} &\sum_{i=0}^{i=N-2} F(\tilde{s}(k+i|k), \tilde{V}(k+i|k)) \\ &- F(\hat{s}(k+i|k-1), V^*(k+i|k-1)) \\ &\leq C_F \cdot \sum_{i=0}^{i=N-2} C_f^i \cdot \bar{\xi} \end{aligned}$$

From *Assumption 3* it yields:

$$\begin{aligned} &E(\tilde{s}(k+N|k)) - E(\hat{s}(k+N-1|k-1)) \\ &= E(\tilde{s}(k+N|k)) - E(\tilde{s}(k+N-1|k)) \\ &+ E(\tilde{s}(k+N-1|k)) - E(\hat{s}(k+N-1|k-1)) \\ &\leq E(\tilde{s}(k+N|k)) - E(\tilde{s}(k+N-1|k)) + C_E C_f^{N-1} \bar{\xi} \end{aligned}$$

We used the instantaneous difference of the predictive state $\hat{s}(k+N-1|k)$ and the feasible state $\tilde{s}(k+N-1|k-1)$ at the time-step $k+N-1$ such that:

$$||\tilde{s}(k+N-1|k-1) - \hat{s}(k+N-1|k)|| \leq C_f^{N-1} \bar{\xi}$$

Therefore, we obtain:

$$\begin{aligned} \Delta J \leq &\left(C_F \sum_{i=0}^{i=N-2} C_f^i + C_E C_f^{N-1} \right) \bar{\xi} + \\ &+ \Big[F(\tilde{s}(k+N-1|k), h(\hat{s}(k+N-1|k))) \\ &+ E(\tilde{s}(k+N|k)) - E(\tilde{s}(k+N-1|k)) \Big] \\ &- F(\hat{s}(k-1|k-1), V^*(k-1|k-1)) \end{aligned}$$

Finally, taking into account the *Assumption 2* and using (14):

$$\begin{aligned}\Delta J &\leq \left(C_F \sum_{i=0}^{i=N-2} C_f^i + C_E C_f^{N-1}\right)\bar{\xi} - \\ &- F(\hat{s}(k-1|k-1), V^*(k-1|k-1)) \\ &\leq \left(C_F \sum_{i=0}^{i=N-2} C_f^i + C_E C_f^{N-1}\right)\bar{\xi} - \\ &- min(q_1, q_2, \cdots, q_{(2n)}, r_1, \cdots, r_6)||\hat{s}(k-1|k-1)||^2\end{aligned}$$

From the optimality of the solution, we derive the following:

$$\Delta J^* = J_N^*(k) - J_N^*(k-1) \leq \Delta J \tag{18}$$

IV. Simulation Results

A free flying pinhole camera wrt a fixed target in the $3D$ cartesian space is assumed for the simulation results. In these simulations we assume that disturbances are affecting the systems and comparisons are made to verify the robustness of the scheme. For all of the presented simulations, the sampling period dt is equal to 0.04. The prediction horizon N as well as the focal length λ are equal to $N = 10$ and $\lambda = 1$ respectively. Also the value of α_{ε_f} is taken to be equal to zero. The target comprised of four feature points on a vertical plane, forming a square with edge 0.1 m. The desired pose of the target wrt the camera frame O_c is $P_{d/O_c} = [0, 0, 0.5, 0, 0, 0]$. The desired image features are: $s^* = [u_1^*, v_1^*, u_2^*, v_2^*, u_3^*, v_3^*, u_4^*, v_4^*] = [-0.2, -0.2, 0.2, -0.2, -0.2, 0.2, 0.2, 0.2]$. The initial pose of the target wrt the camera frame is $P_{init/O_c} = [0.0894, 0.116, 0.6565, -1.3208, 0, -1.9008]$. The initial image features are: $s = [-0.008, 0.017, 0.258, 0.038, -0.009, 0.3413, 0.2774, 0.3332]$. Note that in this configuration the classical IBVS with constant z parameter ($z = z^*$) leads to failure, because during the control operation the image features leaves the image plane. The visibility constraints of the system are defined by (see Fig.2):

$$\begin{bmatrix} \underline{u} = -0.5 \\ \underline{v} = -0.38 \end{bmatrix} \leq \begin{bmatrix} u(t) \\ v(t) \end{bmatrix} \leq \begin{bmatrix} \bar{u} = 0.5 \\ \bar{v} = 0.38 \end{bmatrix} \tag{19}$$

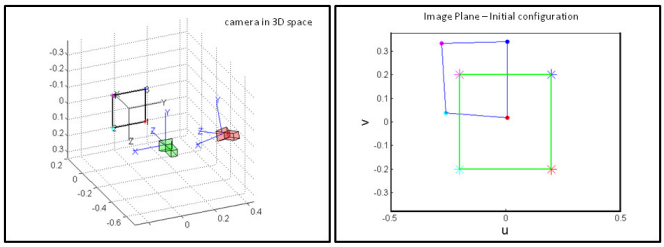

Fig. 2. (a) The initial configuration in 3D space. The initial and desired configuration of the camera are presented by red and green color respectively (b) Image plane at initial time. The initial and desired position of the target on the image plane are denoted by blue and green lines respectively. Note that the target during the control operation should remain in the image plane.

The matrix P is taken to be the identity matrix $I_{8\times 8}$, and the matrices R and Q are defined as $R = diag(0.01, 0.01, 0.01, 0.01, 0.01, 0.01)$ and $Q = diag(5, 5, 5, 5, 5, 5, 5, 5)$. Also the control input is assumed to be bounded by 0.2 m/s for the translational velocity and 0.2 rad/s for the rotational velocity.

A. The case of "constant z"

The Lipschitz constant, using *Lemma1* is calculated as: $C_f = 1.11313708$. In this step we choose $\varepsilon_0 = 0.1$. Considering *Assumption1*, which for each image feature, results in a circle around the desired position of the image feature in image plane with radius equal to 0.025. From *Assumption 3* and 4 we have $C_E = 0.2$ and $\alpha_\varepsilon = 0.01$. Finally, using (17) the allowable upper bound of the disturbances is $\bar{\xi} = 0.01646$. In order to verify that, first we add a perturbation to the system bounded by $\bar{\xi} = 0.01635$ which is smaller than the computed one. It can be witnessed that all image errors in the end of the control operation are smaller than 0.025, thus, the state of the system reaches and is staying inside the desired terminal set. Furthermore, the camera reaches the desired pose in the 3D space, see Fig. 3.

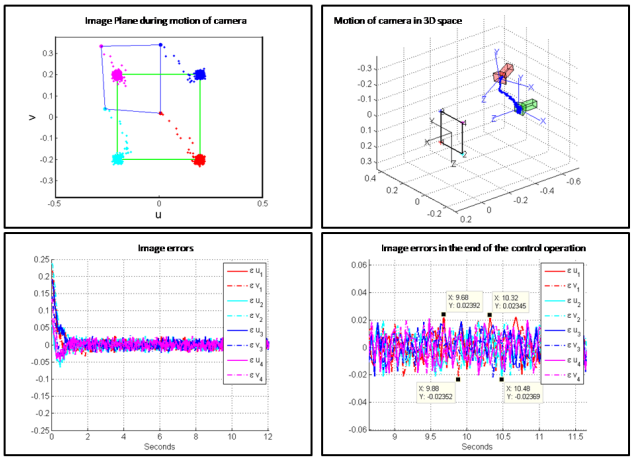

Fig. 3. Response of the *"constant z"* system, under disturbance bounded by $\bar{\xi} = 0.01635$. The camera reaches the desired position in $3d$ space and the image errors will reaches and staying in the expected terminal set.

Let the system to be affected by disturbances bounded by $\bar{\xi} = 0.017$ which is bigger than the computed allowable one. It can be seen that the image errors in the end of the control operation leave the pre-desired terminal set (see Fig. 4). Thus, the simulation verifies our theoretic results.

B. The case of "known z"

Using *Lemma 1* we get: $C_f = 1.11313708$. Choosing $\varepsilon_0 = 0.1$ yields to $C_E = 0.2$ and $\alpha_\varepsilon = 0.01$. the upper bound of the allowable disturbance calculated by (17) is $\bar{w} = 0.01646$. We assume a disturbance affecting the system bounded by $\bar{\xi} = 0.0162$ which is smaller that the computed one. It is evident that all of the image features are reaching and staying in the expected terminal set, see Fig. 5. Adding a bigger disturbance to the system bounded by $\bar{\xi} = 0.0169$ which is bigger than the computed allowable one, the image features fail to stay in the expected terminal set, see Fig 6.

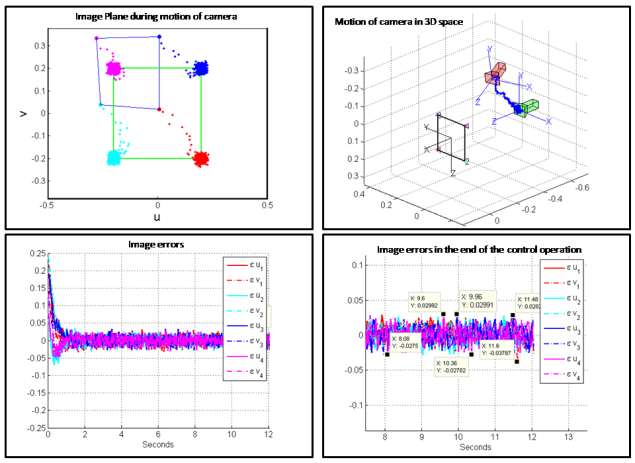

Fig. 4. Response of the *"constant z"* system under disturbance $\bar{\xi} = 0.017$. The image errors are not staying in the expected terminal set.

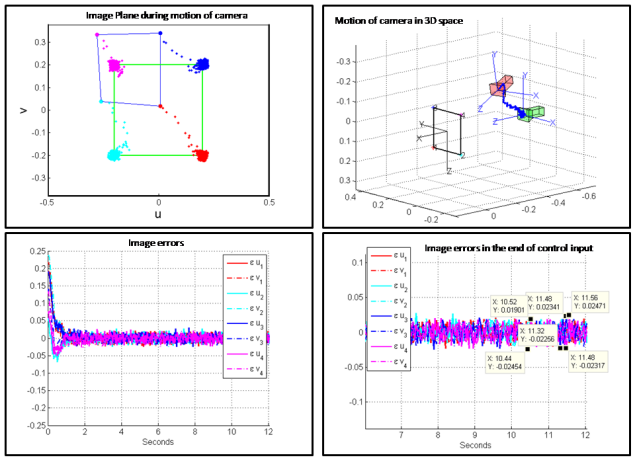

Fig. 5. Response of the *"known z"* system under disturbance $\bar{\xi} = 0.0162$. The camera reached to the desired position in 3d space and the image errors will reach and stay in the expected terminal set.

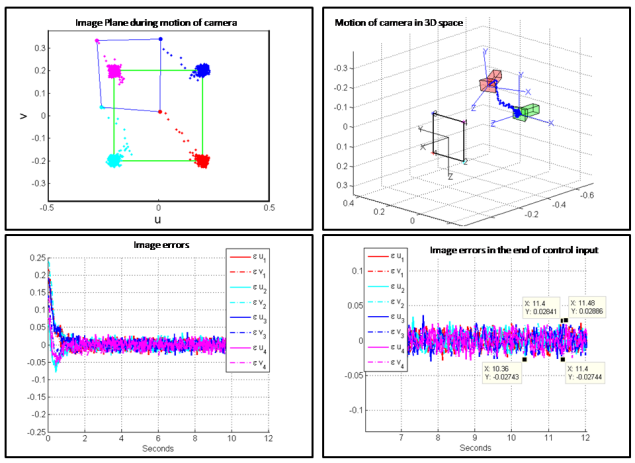

Fig. 6. Response of the *"known z"* system under disturbance $\bar{\xi} = 0.0169$. The image errors did not stay in the expected terminal set.

V. Conclusions

In this paper, an Image Based Visual Servoing via Nonlinear Model Predictive Control framework with robustness analysis was proposed. More particularly, external, bounded, additive disturbances that are affecting the nominal system were considered. The robustness analysis for image based nonlinear predictive controller was conducted and an permissible upper bound for the disturbances was validated. Future work will involve an experimental application that validates the theoretical results.

Acknowledgment

This work was supported by the EU funded project PANDORA: Persistent Autonomy through learNing, aDaptation, Observation and ReplAnning, FP7288273, 20122014.

References

[1] F. Chaumette and S. Hutchinson, "Visual servo control. i. basic approaches," *IEEE Robotics and Automation Magazine*, vol. 13, no. 4, pp. 82–90, 2006.

[2] F. Chaumette and S. Hutchinson, "Visual servo control, part ii: Advanced approaches," *IEEE Robotics and Automation Magazine*, vol. 14, no. 1, pp. 109–118, 2007.

[3] F. Chaumette, "Potential problems of stability and convergence in image-based and position-based visual servoing," pp. 66–78, 1998.

[4] M. Kazemi, K. Gupta, and M. Mehrandezh, "Global path planning for robust visual servoing in complex environments," *Proceedings of the 2009 IEEE International Conference on Robotics and Automation*, pp. 1726–1732, 2009.

[5] Y. Mezouar and F. Chaumette, "Path planning for robust image-based control," *IEEE Transactions on Robotics and Automation*, vol. 18, no. 4, pp. 534–549, 2002.

[6] G. Chesi, "Visual servoing path planning via homogeneous forms and lmi optimizations," *IEEE Transactions on Robotics*, vol. 25, no. 2, pp. 281–291, 2009.

[7] F. Allgwer, R. Findeisen, and Z. Nagy, "Nonlinear model predictive control: From theory to application," *the Chinese Institute of Chemical Engineers*, vol. 35, no. 3, pp. 299–315, 2004.

[8] S. Heshmati-alamdari, A. Eqtami, G. C. Karras, D. V. Dimarogonas, and K. J. Kyriakopoulos, "A self-triggered visual servoing model predictive control scheme for under-actuated underwater robotic vehicles," *Proceedings of the 2014 IEEE International Conference on Robotics and Automation*, 2014.

[9] G. Allibert, E. Courtial, and Y. Tour, "Visual predictive control for manipulators with catadioptric camera," *Proceedings - IEEE International Conference on Robotics and Automation*, pp. 510–515, 2008.

[10] G. Allibert, E. Courtial, and F. Chaumette, "Predictive control for constrained image-based visual servoing," *IEEE Transactions on Robotics*, vol. 26, no. 5, pp. 933–939, 2010.

[11] M. Sauve, P. Poignet, and E. Dombre, "Ultrasound image-based visual servoing of a surgical instrument through nonlinear model predictive control," *International Journal of Robotics Research*, vol. 27, no. 1, pp. 25–40, 2008.

[12] G. Allibert, E. Courtial, and Y. Toure, "Real-time visual predictive controller for image-based trajectory tracking of a mobile robot," *IFAC Proceedings Volumes (IFAC-PapersOnline)*, vol. 17, 2008.

[13] D. Lee, H. Lim, and H. Kim, "Obstacle avoidance using image-based visual servoing integrated with nonlinear model predictive control," *Proceedings of the IEEE Conference on Decision and Control*, pp. 5689–5694, 2011.

[14] E. Malis and P. Rives, "Robustness of image-based visual servoing with respect to depth distribution errors," *Proceedings - IEEE International Conference on Robotics and Automation*, pp. 1056–1061, 2003.

[15] D. L. Marruedo, T. Alamo, and E. Camacho, "Input-to-state stable mpc for constrained discrete-time nonlinear systems with bounded additive uncertainties," *41st IEEE Conf. Decision and Control*, pp. 4619 – 4624, 2002.

[16] G. Pin, D. Raimondo, L. Magni, and T. Parisini, "Robust model predictive control of nonlinear systems with bounded and state-dependent uncertainties," *IEEE Transactions on Automatic Control*, vol. 54, no. 7, pp. 1681 – 1687, 2009.